

**Electron Spin Resonance Spectra and Crystal and Molecular Structures ‡ of Magnetic-dipole Coupled Bis(1,4-dioxane-*O*)bis[*p*-methoxybenzoyl]-trifluoroacetato-*O,O'*]copper(II) Bis(1,4-dioxane) Solvate and catena- $\mu$ -(1,4-Dioxane-*O,O'*)-bis[*p*-nitrobenzoyl]trifluoroacetato-*O,O'*]copper(II)**

Christopher J. Evenhuis, Michael A. Hitchman,\* and Robbie G. McDonald  
Department of Chemistry, University of Tasmania, Box 252C, Hobart, Tasmania 7001, Australia

David M. L. Goodgame

Department of Inorganic Chemistry, Imperial College, South Kensington, London SW7 2AY

Edmund Kwiatkowski and Urszula Dettlaff-Węglikowska

Institute of Chemistry, University of Gdansk, Gdansk 6, Sobieskiego 18, Poland

Chaveng Pakawatchai and Allan H. White †

Department of Physical and Inorganic Chemistry, University of Western Australia, Nedlands, W.A. 6009, Australia

The crystal and molecular structures of the title compounds,  $[\text{Cu}(\text{mbtfac})_2(\text{diox})_2] \cdot 2\text{diox}$  [mbtfac = (*p*-methoxybenzoyl)trifluoroacetate, diox = 1,4-dioxane] and  $[\{\text{Cu}(\text{nbtfac})_2(\text{diox})\}_n]$  [nbtfac = (*p*-nitrobenzoyl)trifluoroacetate] are reported. The former compound belongs to the triclinic space group  $C_1^1$ , with unit-cell parameters  $a = 12.635(4)$ ,  $b = 11.513(3)$ ,  $c = 8.094(3)$  Å,  $\alpha = 70.57(2)^\circ$ ,  $\beta = 81.07(3)^\circ$ ,  $\gamma = 70.47(2)^\circ$ , and  $Z = 1$  and consists of isolated, tetragonally distorted, octahedral molecular units with a pair of *trans* monodentate dioxane ligands and two lattice molecules of dioxane per copper. The latter is monoclinic with unit-cell parameters  $a = 15.753(4)$ ,  $b = 11.262(3)$ ,  $c = 7.587(2)$  Å,  $\beta = 91.72(2)^\circ$ , and  $Z = 2$  and involves a similar copper co-ordination geometry, but with the axial bonds being in this case to bridging dioxane ligands which link the metal ions to form an infinite, one-dimensional polymer. Both compounds show unusual, nine-line e.s.r. spectra when the magnetic field lies parallel or close to the shortest crystal axis. This is interpreted as being caused by a combination of magnetic-dipole coupling with the unpaired electron spins of the copper ions located at  $\pm$  one unit along this axis, and the copper hyperfine interaction, the electron-electron dipolar splitting approximately equalling one-half the hyperfine interaction. In both complexes the electron exchange between the copper ions is slower than the e.s.r. time-scale. The lineshapes and anisotropy of the single-crystal e.s.r. spectra can be satisfactorily simulated using a simple point-dipole model which involves an inter-dipole separation and orientations of the molecular units which are in satisfactory agreement with those suggested by the X-ray structure determinations.

The technique of e.s.r. spectroscopy provides a powerful method of investigating magnetic interactions between transition metal ions. Most work in this area has involved dimers in which the unpaired electrons exchange between the metal centres more rapidly than the time-scale of the e.s.r. measurement. In the case of the most widely studied metal, copper(II), this means that each unpaired electron in the dimer interacts with two nuclei of spin  $I = \frac{3}{2}$ , giving rise to two characteristic seven-line patterns, separated by the so-called zero-field splitting,<sup>1</sup> rather than the simple four-line spectrum observed in the spectrum of an isolated copper(II) ion. Generally, powdered solid or frozen solution spectra have been studied and the probable structures of a wide range of compounds have been deduced using sophisticated computer simulation programs (see ref. 2 for a comprehensive discussion on the e.s.r. spectra of dimers). Magnetic interactions can also significantly affect e.s.r. spectra in the absence of rapid electron exchange, and it is in fact the magnetic dipole coupling with the unpaired electrons of neighbouring paramagnetic centres which causes the relatively broad lines normally observed in the spectra of pure, as opposed to

magnetically dilute, complexes.<sup>3</sup> When the crystal structure of a pure compound is such that each metal has a small number of relatively close paramagnetic neighbours the splittings caused by the magnetic dipole interactions may sometimes be resolved. So far, this has only been reported in a few isolated cases in which the nature of the interaction could be confirmed by measurements made on single crystals.<sup>4-7</sup> However, it is clear that quite complicated lineshapes can occur when the magnitudes of the dipolar and hyperfine splitting parameters bear a simple numerical relationship to one another. Thus, at certain orientations of the magnetic field, the low-temperature e.s.r. spectrum of  $\text{Rb}_2[\text{Cu}(\text{SO}_4)_2] \cdot 6\text{H}_2\text{O}$  shows a pattern of eight lines of relative intensity 1 : 5 : 11 : 15 : 15 : 11 : 5 : 1, this being due to a magnetic dipole interaction with four neighbouring copper(II) ions, the dipolar splitting being equal to that of the hyperfine interaction.<sup>5</sup> Similarly, the e.s.r. spectrum of  $\text{Na}_6[\text{Cu}(\text{P}_2\text{O}_7)_2] \cdot 16\text{H}_2\text{O}$  shows patterns of six and nine lines for various crystal orientations, and this was ascribed<sup>7</sup> to a combination of the hyperfine interaction and a dipolar coupling with two equivalent neighbours.

The observation of anomalous structure in the e.s.r. spectrum of a copper(II) complex might, therefore, be due to either of the above causes. One way of distinguishing between these is by studying the lineshape variation as a function of the magnetic field direction, since the magnetic dipole interaction is highly anisotropic. For those orientations where the magnetic dipole interaction is small, the spectrum of a dimer involving rapid electron exchange should collapse to a seven-

\* Author for information regarding the spectroscopic results.

† Author for information concerning the structural results.

‡ Supplementary data available (No. SUP 23849, 20 pp.): structure factors, thermal parameters, H-atom co-ordinates. See Instructions for Authors, *J. Chem. Soc., Dalton Trans.*, 1984, Issue 1, pp. xvii-xix.

**Table 1.** Non-hydrogen atom co-ordinates for complexes (1) and (2)

Atom	[Cu(nbtfac) <sub>2</sub> (diox) <sub>2</sub> ] <sub>n</sub> (2)			[Cu(mbtfac) <sub>2</sub> (diox) <sub>2</sub> ]-2diox (1)		
	x	y	z	x	y	z
Cu	0	0	0	0	0	0
Ligand						
O(1)	0.1202(2)	0.0295(3)	0.0427(5)	-0.0898(2)	0.1673(3)	-0.1348(4)
C(2)	0.1486(3)	0.1240(5)	0.1097(6)	-0.0478(3)	0.2472(4)	-0.2531(5)
C(21)	0.2418(4)	0.1182(6)	0.1589(9)	-0.1375(4)	0.3694(5)	-0.3388(7)
F(21)	0.2571(3)	0.0333(5)	0.2780(8)	-0.1025(3)	0.4526(3)	-0.4701(5)
F(22)	0.2738(2)	0.2106(5)	0.2353(9)	-0.2138(3)	0.3429(3)	-0.4071(5)
F(23)	0.2891(2)	0.0888(6)	0.0354(6)	-0.1970(3)	0.4287(3)	-0.2266(5)
C(3)	0.1055(3)	0.2272(4)	0.1458(7)	0.0606(3)	0.2364(4)	-0.3064(5)
C(4)	0.0183(3)	0.2429(4)	0.1093(6)	0.1522(3)	0.1290(4)	-0.2346(5)
O(5)	-0.0283(2)	0.1641(3)	0.0405(5)	0.1390(2)	0.0296(3)	-0.1140(4)
C(41)	-0.0263(3)	0.3553(4)	0.1556(6)	0.2687(3)	0.1270(4)	-0.2926(5)
C(42)	0.0153(3)	0.4530(5)	0.2307(7)	0.2963(3)	0.2174(4)	-0.4410(5)
C(43)	-0.0299(4)	0.5526(5)	0.2753(8)	0.4060(3)	0.2131(4)	-0.4929(5)
C(44)	-0.1153(3)	0.5548(4)	0.2420(6)	0.4915(3)	0.1185(4)	-0.3945(5)
N,O(441)	-0.1639(4)	0.6609(4)	0.2933(8)	0.6025(2)	0.1053(3)	-0.4325(4)
O(441A)	-0.2356(3)	0.6720(4)	0.2307(8)			
O(441B)	-0.1327(3)	0.7303(5)	0.3929(9)			
C(442)				0.6349(4)	0.1963(5)	-0.5825(7)
C(45)	-0.1581(3)	0.4616(5)	0.1667(7)	0.4661(3)	0.0274(4)	-0.2459(6)
C(46)	-0.1125(3)	0.3614(4)	0.1258(7)	0.3568(4)	0.0318(4)	-0.1968(5)
Co-ordinated solvent, S						
O(S1)	0.0110(2)	0.0274(3)	-0.3199(5)	0.0161(3)	0.0896(3)	0.2317(4)
C(S2)	0.0788(3)	-0.0199(5)	-0.4204(8)	0.1200(4)	0.0507(5)	0.3125(7)
C(S3)				0.1821(4)	0.1468(5)	0.2296(7)
O(S4)				0.1175(3)	0.2713(3)	0.2390(4)
C(S5)				0.0140(5)	0.3111(5)	0.1586(7)
C(S6)	-0.0459(4)	0.0936(4)	-0.4333(8)	-0.0494(4)	0.2159(6)	0.2401(8)
Unco-ordinated solvent, S'						
O(S'1)				0.4703(4)	0.3120(4)	1.0334(4)
C(S'2)				0.5495(5)	0.3201(6)	0.8878(8)
C(S'3)				0.5176(5)	0.4389(6)	0.7500(8)
O(S'4)				0.4089(3)	0.4668(4)	0.6934(5)
C(S'5)				0.3304(5)	0.4584(7)	0.8355(10)
C(S'6)				0.3626(6)	0.3410(7)	0.9766(9)

line pattern, while when electron exchange is relatively slow, the simple four-line spectrum of an isolated copper(II) should appear. For a typical copper complex having a dipolar coupling of  $ca. 10^{-2} \text{ cm}^{-1}$  spectra due to isolated metal ions should be observed when electron exchange is slower than  $ca. 5 \times 10^8 \text{ s}^{-1}$ .

Recently, Kwiatkowski and co-workers<sup>8</sup> reported the observation of an unusual nine-line splitting pattern in the  $g$  region of the powder e.s.r. spectra of a number of adducts of substituted acetylacetonato-complexes of copper(II). It was tentatively suggested that this pattern might arise if the complexes are dimeric, with a zero-field splitting equal to the copper hyperfine parameter  $A_{II}$ . In order to test this hypothesis, and to investigate in detail how the e.s.r. spectrum is related to the structure of the complexes, we have determined the crystal structure of two representative compounds, bis(1,4-dioxane-*O*)bis[(*p*-methoxybenzoyl)trifluoroacetato-*O,O'*]copper(II) bis(1,4-dioxane) solvate, [Cu(mbtfac)<sub>2</sub>(diox)<sub>2</sub>]-2diox (1), and *catena*- $\mu$ -(1,4-dioxane-*O,O'*)-bis[(*p*-nitrobenzoyl)trifluoroacetato-*O,O'*]copper(II), [Cu(nbtfac)<sub>2</sub>(diox)<sub>2</sub>]<sub>n</sub> (2), and studied the variation of their e.s.r. spectra as a function of crystal orientation. This paper presents the results of these studies, which show that neither complex is in fact dimeric, one being monomeric and the other an infinite polymer. In both cases, electron exchange between the copper(II) ions is slower than the e.s.r. time-scale and the

unusual nine-line pattern is due to a magnetic dipole interaction with two neighbouring copper(II) ions, the splitting of which is equal to half the hyperfine  $A_{II}$  value.

### Experimental

The complexes (1) and (2) were prepared by adding the stoichiometric amount of copper(II) acetate dissolved in hot water to a methanolic solution of the  $\beta$ -diketone, and recrystallising the resultant solid from 1,4-dioxane. In each case large, well formed green crystals were obtained containing 1 mol of dioxane per mol of copper for the complex with the *p*-nitro-substituted ligand, and 4 mol for that with the *p*-methoxy-substituted ligand. Both compounds lose 1,4-dioxane rapidly in air, making accurate analyses impossible. The formulated stoichiometries thus rest solely upon the X-ray structure determinations. These were performed upon crystals mounted in sealed capillaries containing a small amount of solvent. E.s.r. spectra were measured at room temperature using a JEOL JES FE 3X spectrometer operating at X-band frequency. Spectra were also recorded at 105 K for the complex [Cu(mbtfac)<sub>2</sub>(diox)<sub>2</sub>]-2diox (1) and these were indistinguishable in all but intensity from those recorded at room temperature. Crystals were mounted on a quartz rod suspended in a sealed quartz tube containing a small amount of solvent. The crystal rotations were performed using a JEOL

**Table 2.** Copper atom environments. The first column in the matrix is the copper-ligand distance (Å). Other entries are the angles (°) subtended at the copper by the relevant atoms. Italicised atoms are generated by the inversion centre at the copper

Complex (2)	$r_{\text{Cu-O}}$	O(5)	O(S1)	O(I)	O(5)	O(SI)
O(1)	1.940(4)	92.2(1)	92.6(1)	180.0(-)	87.8(1)	87.4(1)
O(5)	1.928(3)		93.5(1)	87.8(1)	180.0(-)	86.5(1)
O(S1)	2.458(4)					180.0(-)
Complex (1)	$r_{\text{Cu-O}}$	O(5)	O(S1)	O(I)	O(5)	O(SI)
O(1)	1.927(2)	92.7(1)	91.0(1)	180.0(-)	87.3(1)	89.0(1)
O(5)	1.933(3)		90.2(1)	87.3(1)	180.0(-)	89.8(1)
O(S1)	2.484(4)					180.0(-)

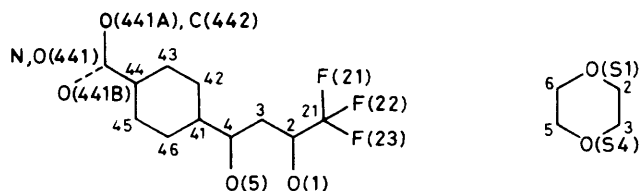
rotation accessory, the initial alignments being carried out using a polarising microscope. Each set of spectra were measured on several different crystals, to check for consistency and to minimize errors in alignment.

**Crystallography.**— $[\{\text{Cu}(\text{nbtfac})_2(\text{diox})\}_n]$  (2)  $\equiv$   $(\text{C}_{24}\text{H}_{18}\text{CuF}_6\text{N}_2\text{O}_{10})_n$ ,  $M = 671.9$ , monoclinic, space group  $P2_1/n$  (variant of  $C_{2h}^5$ , no. 14),  $a = 15.753(4)$ ,  $b = 11.262(3)$ ,  $c = 7.587(2)$  Å,  $\beta = 91.72(2)^\circ$ ,  $U = 1\,345.4(6)$  Å<sup>3</sup>,  $D_c = 1.66$  g cm<sup>-3</sup>,  $Z = 2$ ,  $F(000) = 678$ ,  $\mu_{\text{Mo}} = 8.5$  cm<sup>-1</sup>. Specimen: cuboid, 0.4 mm (capillary).  $2\theta_{\text{max.}} = 45^\circ$ .  $N$ ,  $N_0 = 1\,841$ ,  $1\,405$ .  $R$ ,  $R' = 0.048, 0.062$ .

$[\text{Cu}(\text{mbtfac})_2(\text{diox})_2] \cdot 2\text{diox}$  (1)  $\equiv$   $\text{C}_{38}\text{H}_{48}\text{CuF}_6\text{O}_{14}$ ,  $M = 906.3$ , triclinic ( $C_1^1$ , no. 2),  $a = 12.635(4)$ ,  $b = 11.513(3)$ ,  $c = 8.094(3)$  Å,  $\alpha = 70.57(2)$ ,  $\beta = 81.07(3)$ ,  $\gamma = 70.47(2)^\circ$ ,  $U = 1\,050(2)$  Å<sup>3</sup>.  $D_c = 1.43$  g cm<sup>-3</sup>,  $Z = 1$ ,  $F(000) = 471$ ,  $\mu_{\text{Mo}} = 5.5$  cm<sup>-1</sup>. Specimen:  $0.40 \times 0.20 \times 0.007$  mm.  $2\theta_{\text{max.}} = 40^\circ$ .  $N$ ,  $N_0$  2 346, 1 931.  $R$ ,  $R' = 0.043, 0.057$ .

**Structure Determinations.**—Unique data sets measured with the above  $2\theta_{\text{max.}}$  limits, using a Syntex  $P2_1$  four-circle diffractometer in conventional  $2\theta/\theta$  scan mode and fitted with a monochromatic Mo- $K_\alpha$  radiation source ( $\lambda = 0.7106$ , Å) yielded  $N$  independent reflections,  $N_0$  with  $I > 3\sigma(I)$  being considered 'observed' and used in the (basically)  $9 \times 9$  block-diagonal least-squares refinement after absorption correction. Anisotropic thermal parameters were refined for the non-hydrogen atoms;  $(x, y, z, U_{\text{iso}})_\text{H}$  were constrained at estimated trigonal and tetrahedral values. Residuals  $R, R'$  are quoted at convergence; reflection weights were  $[\sigma^2(F_o) + 0.0005(F_o)^2]^{-1}$ . Neutral-atom scattering factors were used, those for the non-hydrogen atoms being corrected for anomalous dispersion ( $f', f''$ ). Computation used the X-RAY 76 program system implemented by S. R. Hall on a Perkin-Elmer 3240 computer. Atomic co-ordinates are given in Table 1.

Atom labelling within the ligand and solvent species is shown below.

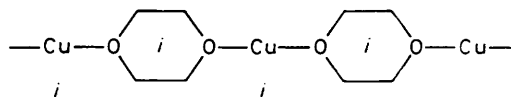


## Results and Discussion

**Structural Commentary.**—In both structures we find a copper(II) atom pseudo-square-planar co-ordinated by a pair of  $O, O'$ -chelating acetylacetonato-ligands, each unsymmetrically substituted at the  $\beta$ -carbon atoms by aromatic and trifluoromethyl moieties (Figures 1 and 2). The asymmetric

unit of each structure comprises only one half of the molecule, the copper atom being disposed on a crystallographic inversion centre (0,0,0), and relating the independent ligand to its inversion image, so that the substituents of the two ligands lie *trans* to each other. The copper atom and its co-ordination sphere derived from the  $\beta$ -diketonate ligand, *i.e.* the  $\text{CuO}_4$  unit, is thus necessarily planar. The conjugated  $\text{C}_3\text{O}_2$   $\beta$ -diketonate systems are each closely coplanar [ $\sigma$  values are 0.002 and 0.007 Å, and copper atom deviations 0.254 and 0.033 Å for (2) and (1), respectively], with dihedral angles to the  $\text{CuO}_4$  planes of 10.9 and 1.4°. The  $\text{C}_6$  skeletons of the aromatic substituent rings make angles of 3.5 and 12.1° to the  $\text{C}_3\text{O}_2$  'plane', while in (2) the nitro-group lies at a dihedral angle of 16.5° for its associated  $\text{C}_6$  aromatic plane.

As indicated by their formulae, there are dioxane molecules of solvation present in each complex, one per  $\text{CuL}_2$  molecule in  $[\{\text{Cu}(\text{nbtfac})_2(\text{diox})\}_n]$  (2) and four in  $[\text{Cu}(\text{mbtfac})_2(\text{diox})_2] \cdot 2\text{diox}$  (1). The dioxane molecules are centrosymmetric about (0,0, $\frac{1}{2}$ ) in the former compound, so that there is only one half solvent molecule per asymmetric unit. The fifth and sixth *trans* co-ordination sites of the copper atom are occupied by long contacts ( $\text{Cu-O}$ , 2.458 Å) to the oxygen atoms of these centrosymmetrically related bidentate dioxane molecules, which thus bridge the copper atoms at successive cell origins along  $c$  [Figure 2(a)] (also see below), in a one-dimensional



polymeric array. In complex (1) *trans* fifth- and sixth-co-ordination sites of the copper atom are occupied by long bonds ( $\text{Cu-O}$ , 2.484 Å) to monodentate dioxane molecules [Figure 2(b)], so that although the  $c$  dimension is comparable to that of the monodioxane adduct, there is an array of independent  $\text{CuL}_2(\text{diox})_2$  species rather than a polymer along  $c$ . This is reflected in the greater inclination of the  $\text{CuO}_4$  plane to the  $c$  axis (26.0 compared with 12.7°). A further solvent pair is incorporated into the structure as an array of centrosymmetrically related species filling the columnar void at the centre of the cell along ( $\frac{1}{2}, \frac{1}{2}, z$ ) [Figure 1(b)]. The chair conformation of the three different types of dioxane present in the two structures is similar to that observed in other metal complexes involving this ligand,<sup>9-12</sup> which also frequently contain dioxane molecules of solvation.<sup>13,14</sup>

The bond distances and angles about the copper(II) ions are listed in Table 2 and the internal ligand dimensions are given in Table 3. The  $\text{Cu-O}$  bond lengths (average value 1.932 Å) are only marginally greater than those in analogous four-coordinate complexes (typically  $\sim 1.92$  Å<sup>15-18</sup>), the effect being considerably less pronounced than that observed in the five-

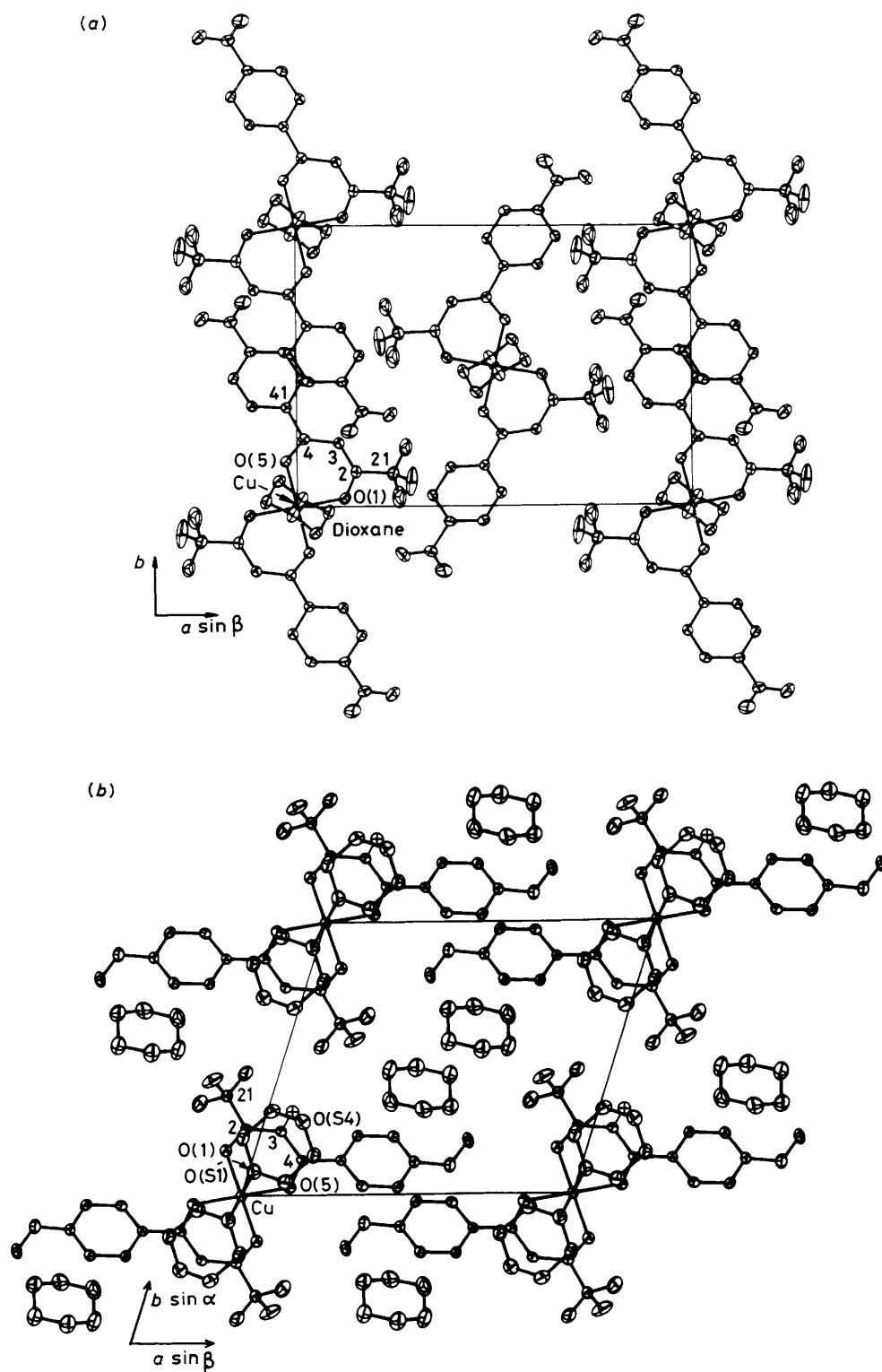


**Figure 1.** Projections of (a)  $[\text{Cu}(\text{nbtfac})_2(\text{diox})]_n$  (2) viewed down the  $c$  axis, and (b)  $[\text{Cu}(\text{mbtfac})_2(\text{diox})_2] \cdot 2\text{diox}$  (1) viewed down the  $c$  axis

co-ordinate adducts formed with nitrogenous bases [in bis(acetylacetonato)(quinoline)copper(II) the average Cu-O distance is 1.95 Å, the axial Cu-N distance being 2.36 Å].<sup>19</sup> Within the  $\text{C}_3\text{O}_2\text{Cu}$   $\beta$ -diketonate systems, the bond lengths are basically equivalent about the  $\gamma$ -carbon atom and typical

of those found in other such complexes;<sup>16-18</sup> nevertheless, significant consistent deviations are observed between C(2)-C(3) and C(3)-C(4), the latter being longer in both complexes. Within the  $\beta$ -diketonate rings, there is a consistent and considerable asymmetry in the angles at the oxygen atoms

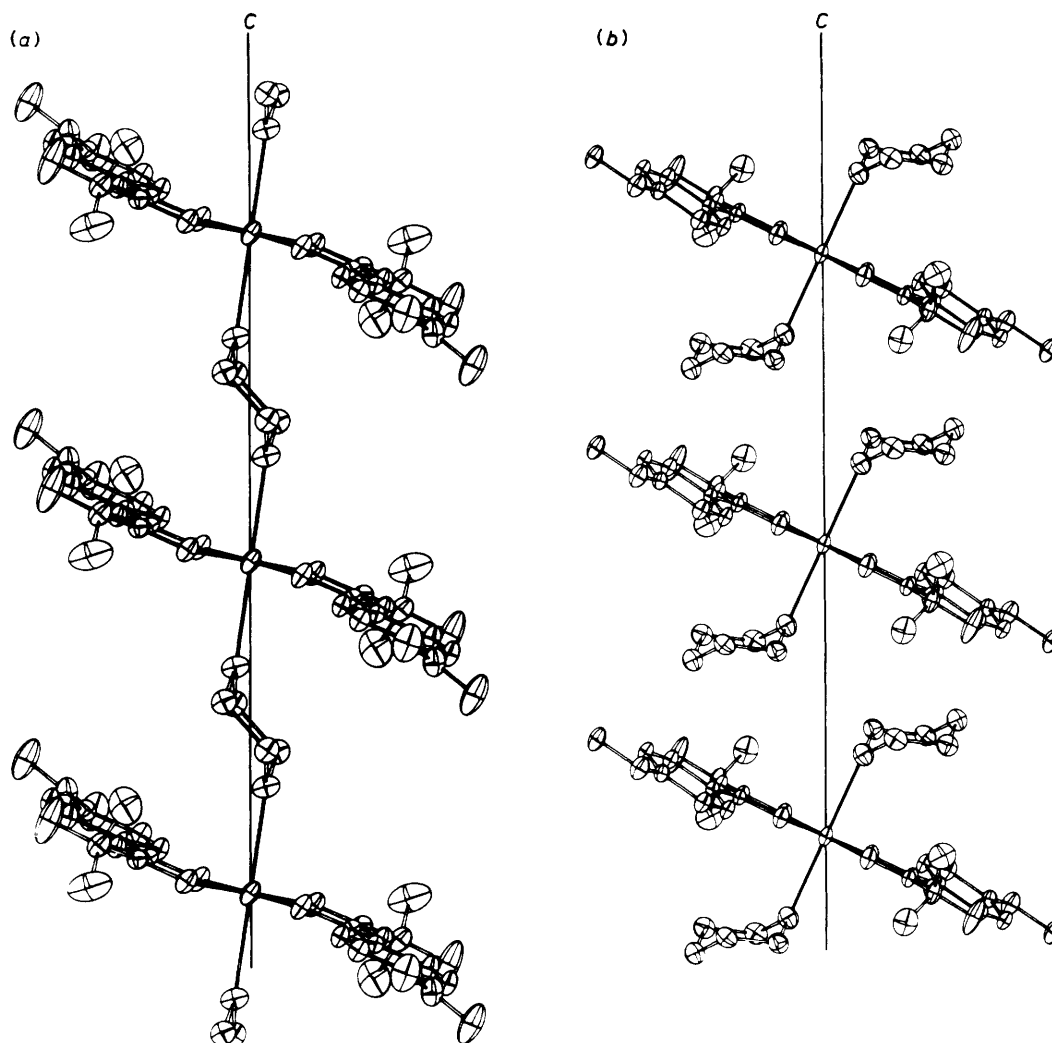


**Figure 2.** (a) View of  $[\{\text{Cu}(\text{nbtfac})_2(\text{diox})\}_n]$  (2) looking down the normal to the plane containing the  $c$  axis and the bisector of the chelate rings. (b) View of the  $[\text{Cu}(\text{mbtfac})_2(\text{diox})_2]$  molecular units of (1) looking down the normal to the plane containing the  $c$  axis and the bisector of the chelate rings. This approximates quite closely the (100) plane for which e.s.r. spectra are shown in Figure 3. The clathrated solvent molecules are omitted for the sake of clarity

and between the angles at C(2) and C(4). Considerable asymmetry is found also in the exocyclic angles at these carbon atoms; in each case the larger of the two is that enclosed by the substituent and C(3). These appear to be associated with interactions between H(3) and one of the  $\text{CF}_3$  fluorine atoms. In both structures the  $\text{CF}_3$  disposition is such that one of the fluorine atoms lies pseudo-coplanar with the  $\beta$ -diketonate ring and close to H(3), probably a consequence of fluorine-oxygen atom repulsions [in (2), F(21B) deviates from the plane by 0.08 Å and lies 2.35 Å from H(3), while in (1), F(21A) is 0.09 Å out of plane and 2.34 Å from H(3)]. In each case the aromatic ring plane is pseudo-coplanar with the  $\beta$ -diketonate ring and contacts between the *ortho*-hydrogen atoms and H(3) are probably responsible for the exocyclic angular asymmetry at C(4).

**E.S.R. Spectra.**—(a)  $[\text{Cu}(\text{mbtfac})_2(\text{diox})_2] \cdot 2\text{diox}$  (1). This complex crystallizes with the (100) crystal face well developed, and spectra were measured at 10° intervals for rotations of crystals about the normal to each crystal face. The rotation about the  $c^*$  axis produced a single broad line for each crystal orientation. The rotations about  $a^*$  and  $b^*$  produced spectra

which were quite similar to one another, with the single line observed when the magnetic field was normal to the  $c$  axis splitting into first four, and then nine lines as the magnetic field approached  $c$ . The orientation of the molecular units of (1) is such that the  $z$  molecular axis (defined as the normal to the  $\text{CuO}_4$  plane formed by the copper and diketonato-oxygen atoms) lies almost exactly in the (100) crystal plane, at an angle of 23° to the  $c$  crystal axis [Figure 2(b)]. The spectra observed for the rotation of the magnetic field in this crystal plane are shown in Figure 3, measured at 10° intervals from the  $z$  molecular axis, this being assumed to coincide with the direction in which the maximum  $g$  value occurred. A positive rotation is defined so that the magnetic field is carried away from the  $c$  axis.

As the triclinic unit cell contains a single molecule, each spectrum is associated with just one molecular orientation. It is noteworthy that the set of spectra are markedly asymmetric with respect to the direction of the angular rotation. Thus, the spectra at  $\sim +30^\circ$  to the  $z$  axis show four well resolved lines of equal intensity, while those at  $-30^\circ$  show nine lines, the outer two lines being about half as intense as the inner seven (Figure 3). The four-line pattern clearly corresponds to the

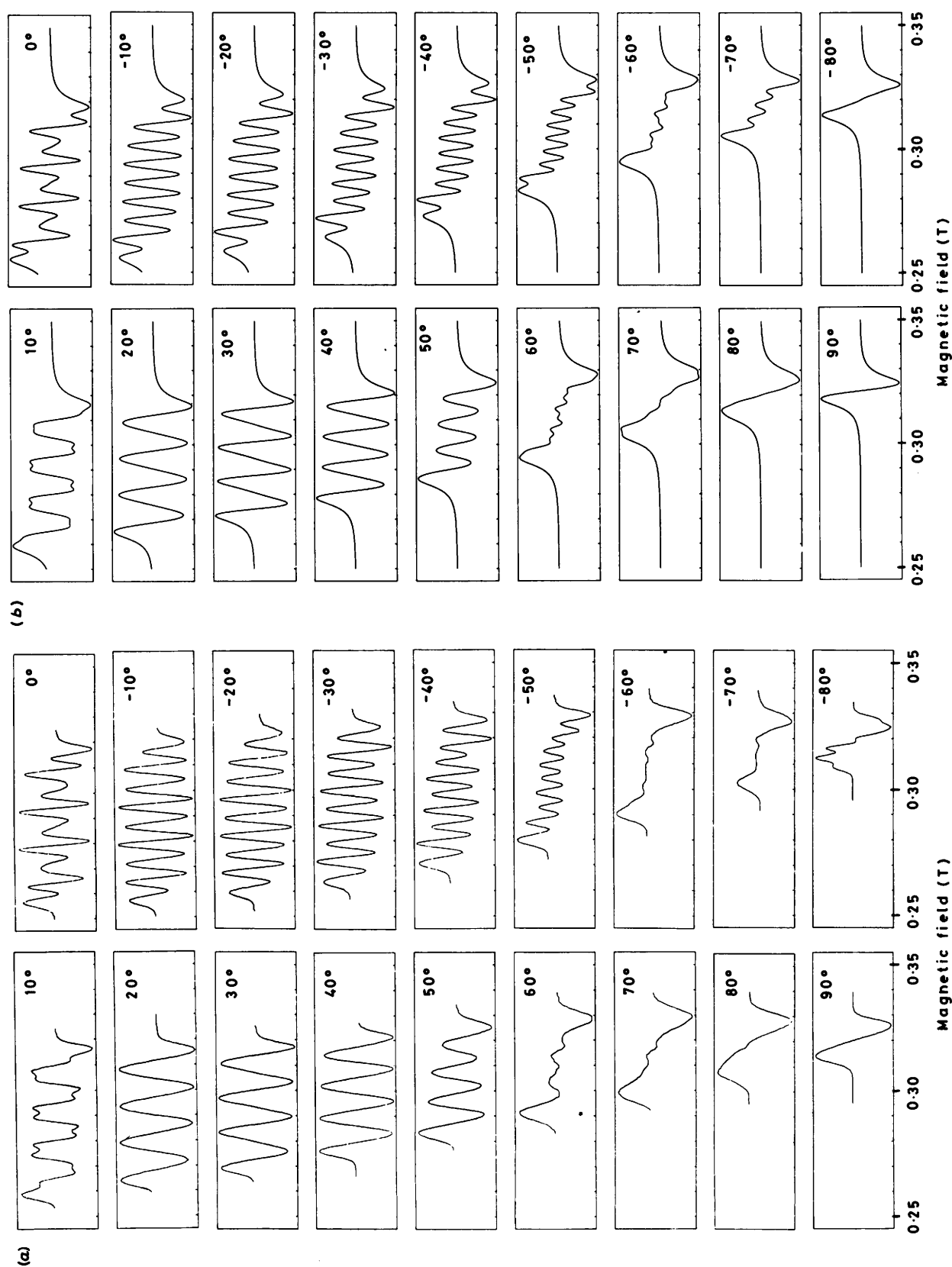


Figure 3. Observed (a) and computer simulated (b) e.s.r. spectra of  $[\text{Cu}(\text{mfac})(\text{diox})_2] \cdot 2\text{diox}$  (I) for the rotation of the crystal in the (100) plane. The angles ( $\theta$ ) define the position of the magnetic field with respect to the  $z$  molecular axis, a positive rotation being away from the  $c$  axis. The simulations were carried out as described in the text, and are for an inter-dipole separation of 8.2 Å and an angle between the inter-dipole vector and the molecular  $z$  axis of  $23^\circ$ .

**Table 3.** Ligand non-hydrogen atom geometries; distance (Å) and angles (°)

	(2)	(1)		(2)	(1)
O(1)-C(2)	1.256(6)	1.275(5)	Co-ordinated solvent		
C(2)-C(3)	1.378(7)	1.348(6)	O(S1)-C(S2)	1.433(7)	1.425(7)
C(2)-C(21)	1.507(8)	1.508(5)	C(S2)-C(S3)	1.469(8)	1.487(8)
C(21)-F(21)	1.332(9)	1.305(6)	C(S3)-O(S4)		1.414(6)
C(21)-F(22)	1.287(8)	1.343(8)	O(S4)-C(S5)		1.418(7)
C(21)-F(23)	1.258(8)	1.309(7)	C(S5)-C(S6)		1.489(9)
C(3)-C(4)	1.404(7)	1.408(5)	C(S6)-O(S1)	1.433(7)	1.431(7)
C(4)-O(5)	1.255(6)	1.275(5)			
C(4)-C(41)	1.495(7)	1.469(6)	Cu-O(S1)-C(S2)	123.6(3)	120.6(3)
C(41)-C(42)	1.393(7)	1.389(5)	Cu-O(S1)-C(S6)	126.6(3)	123.6(3)
C(42)-C(43)	1.377(8)	1.374(6)	C(S2)-O(S1)-C(S6)	109.7(4)	109.9(5)
C(43)-C(44)	1.362(8)	1.376(5)	O(S1)-C(S2)-C(S3)	111.1(4)	110.7(4)
C(44)-N,O(441) *	1.477(7)	1.356(5)	C(S2)-C(S3)-O(S4)		111.5(4)
C(44)-C(45)	1.364(7)	1.384(6)	C(S3)-O(S4)-C(S5)		110.2(5)
C(45)-C(46)	1.378(7)	1.366(6)	O(S4)-C(S5)-C(S6)		111.0(4)
C(41)-C(46)	1.372(7)	1.389(5)	C(S5)-C(S6)-O(S1)	111.1(4)	111.2(4)
O(1)···O(5)	2.682(5)	2.794(4)			
			Unco-ordinated solvent		
Cu-O(1)-C(2)	123.1(3)	123.0(2)	O(S'1)-C(S'2)		1.422(7)
Cu-O(5)-C(4)	127.5(3)	128.2(2)	C(S'2)-C(S'3)		1.426(8)
O(1)-C(2)-C(3)	128.6(5)	129.5(3)	C(S'3)-O(S'4)		1.416(8)
O(1)-C(2)-C(21)	113.5(5)	111.7(3)	O(S'4)-C(S'5)		1.397(8)
C(3)-C(2)-C(21)	118.0(5)	118.8(3)	C(S'5)-C(S'6)		1.430(9)
C(2)-C(21)-F(21)	110.7(5)	115.6(4)	O(S'1)-C(S'6)		1.401(9)
C(2)-C(21)-F(22)	116.4(5)	110.9(4)			
C(2)-C(21)-F(23)	114.9(5)	112.6(4)	C(S'6)-O(S'1)-C(S'2)		110.1(5)
F(21)-C(21)-F(22)	102.4(6)	104.2(4)	O(S'1)-C(S'2)-C(S'3)		113.7(5)
F(21)-C(21)-F(23)	102.6(6)	108.8(4)	C(S'2)-C(S'3)-O(S'4)		112.4(6)
F(22)-C(21)-F(23)	108.4(6)	103.8(4)	C(S'3)-O(S'4)-C(S'5)		110.8(5)
C(2)-C(3)-C(4)	123.4(5)	124.4(3)	O(S'4)-C(S'5)-C(S'6)		114.2(5)
C(3)-C(4)-C(41)	121.6(4)	121.4(3)	C(S'5)-C(S'6)-O(S'1)		113.7(7)
C(3)-C(4)-O(5)	123.4(4)	122.1(4)			
O(5)-C(4)-C(41)	115.0(4)	116.5(3)			
C(4)-C(41)-C(42)	123.1(4)	123.0(3)			
C(4)-C(41)-C(46)	118.2(4)	119.8(3)			
C(42)-C(41)-C(46)	118.6(4)	117.3(4)			
C(41)-C(42)-C(43)	120.3(5)	121.8(3)			
C(42)-C(43)-C(44)	119.0(5)	119.6(4)			
C(43)-C(44)-C(45)	122.5(5)	119.6(4)			
C(43)-C(44)-N,O(441)	118.9(5)	124.7(4)			
C(45)-C(44)-N,O(441)	118.7(5)	115.7(3)			
C(44)-C(45)-C(46)	118.1(5)	120.2(3)			
C(41)-C(46)-C(45)	121.6(5)	121.4(4)			

\* In (2): N(441)-O(441A,B), 1.218(8), 1.184(8) Å; O(441A)-N(441)-O(441B), 122.9(6)°; C(44)-N(441)-O(441A,B) 117.5(5), 119.6(5)°. In (1): O(441)-C(442) 1.423(6) Å; C(44)-O(441)-C(442) 118.8(3)°.

interaction of an unpaired electron with the nuclear spin of a single copper(II) ion ( $I = \frac{3}{2}$ ), in agreement with the fact that isolated molecular units are present in the crystal. The nine-line pattern is observed when the magnetic field is parallel or close to the  $c$  crystal axis. This is the shortest crystal axis, and a potential source of the observed spectral pattern is magnetic dipole coupling with the unpaired electron spins associated with the two copper(II) ions located at  $\pm 1$  unit-cell dimension along this direction. This effect is exactly analogous to the through-space coupling commonly observed in n.m.r. spectroscopy,<sup>20</sup> except that electron rather than nuclear spins are involved. The interaction with two equivalent neighbours will split each copper line into three components with intensities in the ratio 1 : 2 : 1 as illustrated in Figure 4. The magnetic dipole splitting  $d$  is highly anisotropic with respect to the angle  $\phi$  between the magnetic field direction and the metal-metal vector. Provided that the observed dipolar splittings are small compared with the applied magnetic field, as in the present case, the dipolar coupling  $d$ , in Tesla, is given to a good approximation by equation (i),<sup>21</sup> where  $g$  is the  $g$  value of the complex, and  $r$  is the inter-dipole separation in Å.

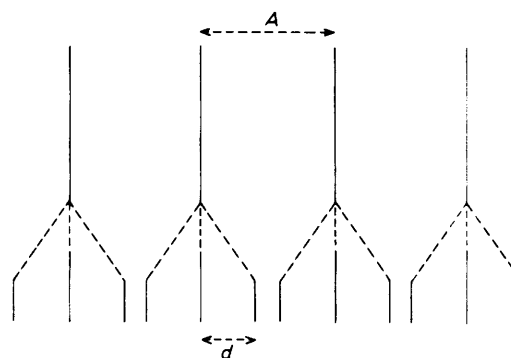


**Figure 4.** Splitting pattern for the e.s.r. spectrum of an unpaired electron interacting with a nuclear spin  $I = \frac{3}{2}$  to give a hyperfine splitting  $A$ , and two equivalent electron spins producing a dipolar splitting  $d$

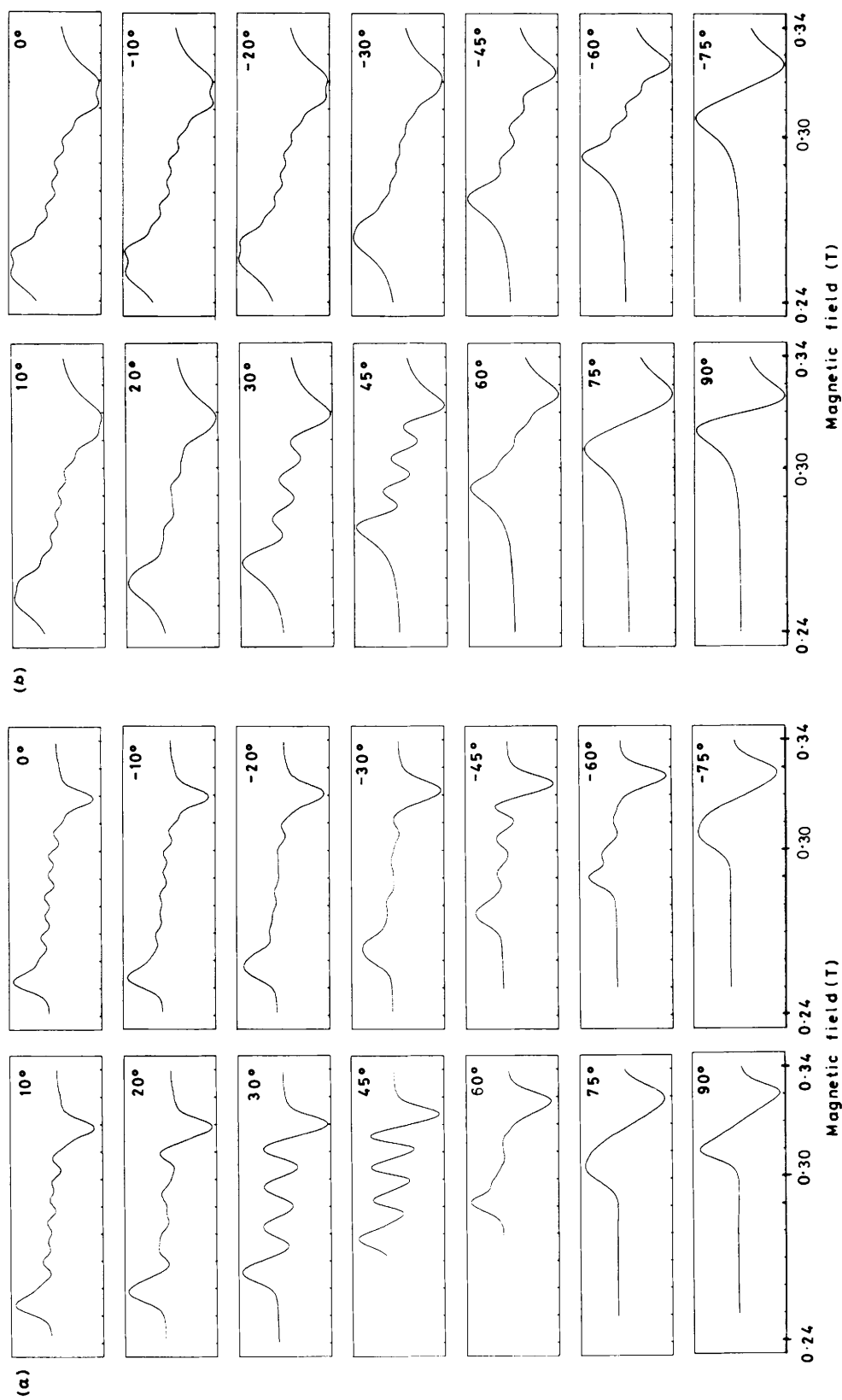


Figure 5. Observed (a) and computer simulated (b) e.s.r. spectra of  $[\text{Cu}(\text{nbfac})_2(\text{diox})_2]_n$  (2) for the rotation of the crystal in the (010) plane. The angles ( $\theta$ ) define the position of the magnetic field with respect to the  $z$  molecular axis, a positive rotation being away from the  $c$  axis. The simulations were carried out as described in the text, and are for an inter-dipole distance of 7.9 Å and an angle between the inter-dipole vector and the molecular  $z$  axis of  $7^\circ$ .



$$d = 0.9274 g (1 - 3 \cos^2 \varphi) / r^3 \quad (i)$$

In general, the above model predicts the observation of twelve lines, and indeed twelve poorly resolved lines are observed when the magnetic field lies at  $\sim 10^\circ$  to the  $z$  axis (Figure 3; note that each inflexion corresponds to a resonance line on a derivative spectrum). However, if the dipolar splitting  $d$  happens to be approximately equal to half the hyperfine splitting  $A$ , then a nine-line pattern is expected, with the outer two lines having half the intensity of the inner seven (Figure 4). Moreover, the dipolar splitting vanishes when  $\varphi = 54.7^\circ$  [equation (i)] so that when the magnetic field makes this angle with the inter-dipole vector only the metal hyperfine splitting should remain. In the present case, since the  $z$  molecular axis lies  $23^\circ$  from the metal-metal direction, the dipolar coupling should vanish at an angle  $\theta \approx 54.7 - 23 = 31.7^\circ$ , as indeed observed experimentally (Figure 3).

To obtain a more quantitative interpretation of the spectra a computer program was written to simulate the spectra predicted by the above model. The  $g$  values were represented by equation (ii), with  $g_{\parallel}$  and  $g_{\perp}$  being set equal to the maximum and minimum observed values,  $g_{\parallel} = 2.310$ ,  $g_{\perp} = 2.064$ . The magnitudes of the hyperfine splittings were represented by equation (iii), with the values of  $A_{\parallel}$  and  $A_{\perp}$  being set equal to

$$g = (g_{\parallel}^2 \cos^2 \theta + g_{\perp}^2 \sin^2 \theta)^{\frac{1}{2}} \quad (ii)$$

$$A = (g_{\parallel}^2 A_{\parallel}^2 \cos^2 \theta + g_{\perp}^2 A_{\perp}^2 \sin^2 \theta)^{\frac{1}{2}} \quad (iii)$$

those observed in dioxane solution,  $1.5 \times 10^{-2}$  and  $7.0 \times 10^{-4}$  T, respectively. A Lorentzian lineshape for the component peaks was assumed,<sup>22</sup> the half-width at half-height being set constant at  $4.0 \times 10^{-3}$  T. The slightly different hyperfine splitting expected for the two isotopes of copper was taken into account;<sup>5</sup> the values given above refer to the more abundant isotope. Spectra were simulated for various possible values of the interdipole distance  $r$  and the angle between the molecular  $z$  axis and the dipole-dipole vector  $\eta$ . The calculated spectra were found to be quite sensitive to both these parameters and optimum agreement with experiment was obtained for the values  $r = 8.2 \pm 0.2$  Å and  $\eta = 23 \pm 2^\circ$ , the error limits indicating the amount by which each parameter must be varied to worsen this agreement significantly. The simulated and experimental spectra agree quite well for almost all values of  $\theta$  (Figure 3) and the best-fit values of  $r$  and  $\eta$  coincide almost exactly with the copper-copper distance deduced from the X-ray structure determination (8.09 Å) and the angle between the  $c$  axis and the  $\text{CuO}_4$  plane formed by the acetylacetonate ligands ( $23^\circ$ ). (In fact, the e.s.r. simulation studies were carried out before the crystallographic data were available.)

(b)  $[\{\text{Cu}(\text{nbtfac})_2(\text{diox})\}_n]$  (2). This complex crystallizes with the (001), (110), and  $(\bar{1}10)$  crystal faces well developed, and spectra were recorded for rotations in the (010), (011), and (0 $\bar{1}$ 1) crystal planes. The monoclinic unit cell of this compound contains two molecules, related by a mirror plane normal to the  $b$  axis, and the spectra observed for the latter two rotations were complicated by the overlapping of the signals due to the different orientations of the two molecules. The spectra for the rotation in the (010) plane, in which the two molecules have equivalent orientations with respect to the applied magnetic field, are shown in Figure 5. The general pattern is broadly similar to that observed for (1) suggesting that despite the very different dioxane co-ordination, a broadly similar mechanism produces the unusual structure in the spectra of both complexes. Thus, nine lines are observed when the magnetic field is parallel to the short (7.6 Å)  $c$  axis, these collapsing to four lines at  $\sim 45^\circ$  to this axis and a single line

at  $\sim \pm 90^\circ$ . However, in (2) the nine-line structure is rather poorly resolved. The four-line pattern clearly suggests that the electron exchange between the metal ions is slower than the e.s.r. time-scale, despite the fact that in this complex the copper ions are linked by dioxane groups (rapid electron exchange would cause a single 'exchange narrowed' peak in an infinite polymer of this type). The relatively slow exchange rate, which is consistent with the observed magnetic behaviour of the compound,<sup>8</sup> is probably related to the fact that the bridging ligands occupy co-ordination sites which are orthogonal to the  $d_{x^2-y^2}$  orbitals containing the unpaired electrons. In agreement with the apparent absence of significant electron exchange, no signal was observed for this or the previous compound in the region ( $\sim 0.15$  T) in which the characteristic  $\Delta M_S = 2$  absorption is observed in typical copper(II) dimers.<sup>2</sup> In contrast to the set of spectra of the (100) plane of (1) those of (2) are quite symmetrical with respect to the sense of the rotation in the (010) plane (Figures 3 and 5). This is because the maximum projection made by the  $z$  molecular axis on the (100) plane makes only a small angle ( $7^\circ$ ) with the  $c$  crystal axis, in contrast to the much larger angle ( $23^\circ$ ) in (1).

Spectral simulations analogous to those described above were carried out for complex (2) using the parameters  $g_{\parallel} = 2.327$ ,  $g_{\perp} = 2.073$ ,  $A_{\parallel} = 1.55 \times 10^{-2}$  T,  $A_{\perp} = 7.0 \times 10^{-4}$  T and half-width  $\Delta B = 8.5 \times 10^{-3}$  T and the experimental and calculated spectra are shown in Figure 5. The fact that a considerably greater half-width was required to optimize the spectral fit than was the case for complex (1) ( $\Delta B = 4.0 \times 10^{-3}$  T) is consistent with the greater density of copper(II) ions per unit volume in (2). The second-closest metal-metal separation in the latter compound, that to the copper at (0.5, 0.5, 0.5), occurs at 10.4 Å, compared with 11.5 Å in the former complex. The optimum values of the inter-dipole separation and angle between the dipole-dipole vector and the  $z$  molecular axis were found to be  $7.9 \pm 0.2$  Å and  $7 \pm 2^\circ$  in reasonable agreement with the values 7.59 Å and  $7^\circ$  suggested by the X-ray structural analysis.

## Conclusions

It is apparent that the simple point-dipole approximation provides a quite satisfactory explanation of the unusual structure observed in the e.s.r. spectra of  $[\text{Cu}(\text{mbtfac})_2(\text{diox})_2] \cdot 2\text{diox}$  (1) and  $[\{\text{Cu}(\text{nbtfac})_2(\text{diox})\}_n]$  (2). This is in contrast to the only other two copper(II) complexes for which magnetic dipole-coupling with slow electron exchange has been reported to modify the e.s.r. spectra. For  $\text{Rb}_2[\text{Cu}(\text{SO}_4)_2] \cdot 6\text{H}_2\text{O}$  it was found necessary to take into account deviations from the point-charge description,<sup>5</sup> while for  $\text{Na}_6[\text{Cu}(\text{P}_2\text{O}_7)_2] \cdot 16\text{H}_2\text{O}$  the spectra could not be explained satisfactorily without including various combinations of the hyperfine states of the neighbouring ions.<sup>7</sup> This may be because the closest metal-metal separations in these latter two compounds, 6.2 and 6.8 Å, are considerably shorter than those in the present complexes ( $\sim 8$  Å). It is interesting to note the particular structural features of the dioxane adducts which underlie their unusual e.s.r. spectra as these might be valuable in predicting other compounds showing similar effects. First, one copper-copper distance is significantly shorter than all others, with the copper-copper vectors and  $z$  molecular axes (and hence the largest hyperfine values) being approximately coincident. Secondly, all molecules in the unit cell have similar orientations (triclinic systems should nearly always satisfy this condition).

The characteristic seven-line spectra, modified by zero-field splittings, observed for copper dimers having relatively rapid electron exchange between the metal ions have often been used to deduce the likely geometries and metal-metal separations

in compounds of this type.<sup>2</sup> Moreover, it has been pointed out<sup>23</sup> that this may be particularly valuable in elucidating the structures of molecules of biological importance containing more than one copper(II) ion. The present study shows that unusual e.s.r. spectra may also occur when copper(II) ions are in relatively close proximity but with the unpaired electrons exchanging between these less rapidly than the e.s.r. time-scale. The spectra then consist of a splitting due to the dipolar coupling between the electron spins superimposed upon the familiar four-line spectrum caused by the copper hyperfine interaction. Both the magnitude and the anisotropy of the dipolar splitting may be explained satisfactorily using a simple point-dipole approximation, so that an investigation of the e.s.r. spectra of this type of system also has the potential to provide information on the distribution of the active centres in large molecules containing two or more paramagnetic metal ions.

### Acknowledgements

The financial support of the Australian Research Grants Commission (to M. A. H. and A. H. W.) is gratefully acknowledged. The Central Science Laboratory of the University of Tasmania is thanked for providing the facilities for the e.s.r. measurements.

### References

- 1 A. Abragam and B. Bleaney, 'Electron Paramagnetic Resonance of Transition Ions,' Clarendon Press, Oxford, 1970, p. 508.
- 2 T. D. Smith and J. R. Pilbrow, *Coord. Chem. Rev.*, 1974, **13**, 173.
- 3 Ref. 1, p. 521.
- 4 Ref. 1, p. 524.
- 5 M. A. Hitchman, *J. Chem. Phys.*, 1978, **68**, 3425.
- 6 G. D. Simpson, R. L. Belford, and R. Biagioni, *Inorg. Chem.*, 1978, **17**, 2424.
- 7 H. So, G. P. Haight, jun., and R. L. Belford, *J. Phys. Chem.*, 1980, **84**, 1849.
- 8 E. Kwiatkowski, Z. Pepliński, and U. Dettlaff-Weglikowska, Proc. 21st Int. Conf. Coord. Chem., Toulouse, France, 1980, p. 376; E. Kwiatkowski and P. Zbigniew, *Transition. Metal Chem.*, 1978, **3**, 305.
- 9 W. S. Dickmann, G. Hamer, S. C. Nyburg, and W. F. Reynolds, *Chem. Commun.*, 1970, 1295.
- 10 M. Frey, *Acta Crystallogr.*, 1971, **27**, 2487.
- 11 J. C. Barnes and T. J. R. Weakley, *Acta Crystallogr., Sect. B*, 1977, **33**, 921.
- 12 J. C. Barnes and L. J. Sesay, *Inorg. Nucl. Chem. Lett.*, 1977, **13**, 153.
- 13 J. C. Barnes and T. J. R. Weakley, *J. Chem. Soc., Dalton Trans.*, 1976, 1786.
- 14 J. C. Barnes and L. J. Sesay, *Acta Crystallogr., Sect. A*, 1975, **31**, 5144.
- 15 B. J. Hathaway and D. E. Billing, *Coord. Chem. Rev.*, 1970, **5**, 143.
- 16 T. S. Piper and R. L. Belford, *Mol. Phys.*, 1962, **5**, 169.
- 17 P. K. Hon, C. E. Pfluger, and R. L. Belford, *Inorg. Chem.*, 1966, **5**, 516.
- 18 J. W. Carmichael, jun., L. K. Steinrauf, and R. L. Belford, *J. Chem. Phys.*, 1965, **43**, 3959.
- 19 P. Jose, S. Ooi, and Q. Fernando, *J. Inorg. Nucl. Chem.*, 1969, **31**, 1971.
- 20 See, for example, A. Carrington and A. D. McLachlan, 'Introduction to Magnetic Resonance,' Harper and Row, New York, 1967, ch. 3.
- 21 Ref. 1, pp. 493, 521-527.
- 22 Ref. 1, p. 58.
- 23 Ref. 2, p. 264.

Received 12th July 1983; Paper 3/1198